

Fluctuations and Correlations of Conserved Charges in QCD at Finite Temperature with Effective Models

Wei-jie Fu,^{1,*} Yu-xin Liu,^{2,3,†} and Yue-Liang Wu^{1,‡}

¹*Kavli Institute for Theoretical Physics China (KITPC),*

*Key Laboratory of Frontiers in Theoretical Physics, Institute of Theoretical Physics,
Chinese Academy of Science, Beijing 100190, China*

²*Department of Physics and State Key Laboratory of Nuclear Physics and Technology,
Peking University, Beijing 100871, China*

³*Center of Theoretical Nuclear Physics,
National Laboratory of Heavy Ion Accelerator, Lanzhou 730000, China*

(Dated: February 22, 2024)

Abstract

We study fluctuations of conserved charges including baryon number, electric charge, and strangeness as well as the correlations among these conserved charges in the 2+1 flavor Polyakov–Nambu–Jona-Lasinio model at finite temperature. The calculated results are compared with those obtained from recent lattice calculations performed with an improved staggered fermion action at two values of the lattice cutoff with almost physical up and down quark masses and a physical value for the strange quark mass. We find that our calculated results are well consistent with those obtained in lattice calculations except for some quantitative differences for fluctuations related with strange quarks. Our calculations indicate that there is a pronounced cusp in the ratio of the quartic to quadratic fluctuations of baryon number, i.e. χ_4^B/χ_2^B , at the critical temperature during the phase transition, which confirms that χ_4^B/χ_2^B is a useful probe of the deconfinement and chiral phase transition.

PACS numbers: 25.75.Nq, 12.38.Mh, 11.30.Rd, 12.38.Gc,

*wjfu@itp.ac.cn

†yxliu@pku.edu.cn

‡ylwu@itp.ac.cn

I. INTRODUCTION

QCD thermodynamics, for example the equation of state of the quark gluon plasma (QGP), phase transition of the chiral symmetry restoration, the deconfinement phase transition and so on, has been a subject of intensive investigation in recent years. On the one hand, the deconfined QGP are expected to be formed in ultrarelativistic heavy-ion collisions [1–8] (for example the current experiments at the Relativistic Heavy Ion Collider (RHIC) and the upcoming experiments at the Large Hadron Collider (LHC)) and in the interior of neutron stars [9–12]; On the other hand, studying the thermodynamical and hydrodynamical behaviors of the QGP, especially the deconfinement and chiral phase transitions, is an elementary problem in strong interaction physics.

Lattice QCD simulation is a principal approach to explore the properties of strongly interacting matter and its deconfinement and chiral phase transitions. In the past years, this method has provided us with lots of information about the QCD thermodynamics and phase transition from the confined hadronic phase to the deconfined QGP one at finite temperature and limited chemical potential (see, for example, Ref. [13–29]). In response to the lattice QCD simulations, many effective models have been developed to describe the behavior and properties of strongly interacting matter, give physical interpretation of the available lattice data, and further to make predictions in the regions of phase diagram that can not be reached by the lattice calculations. The validity of these effective models is expected, since what governs the critical behavior of the QCD phase transition is the universality class of the chiral symmetry which is kept in these effective models.

It has been known that fluctuations of conserved charges, for example the baryon number, electric charge, and strangeness, are particularly sensitive to the structure and behavior of the thermal strongly interacting matter [30–32]. Enhanced fluctuations are close related with the critical behavior of the QCD thermodynamics and phase transitions [33]. Furthermore, the fluctuations and correlations of conserved charges and their high order cumulants provide information about the degrees of freedom (confined hadrons or deconfined QGP) of strongly interacting matter at high temperature [34, 35], thus they are useful probes of the deconfinement and chiral phase evolution [24–28, 36]. More important, the fluctuations and correlations of conserved charges can be extracted not only theoretically from the lattice QCD simulations and effective model calculations but also experimentally from

event-by-event fluctuations [32, 35, 37].

In this work, we will study the fluctuations and correlations of conserved charges and their high order cumulants in the 2+1 flavor Polyakov–Nambu–Jona-Lasinio (PNJL) model [38]. Compared with the conventional Nambu–Jona-Lasinio model, the PNJL model not only has the chiral symmetry as well as the dynamical breaking mechanism of this symmetry, but also include the effect of color confinement through the Polyakov loop [39–47]. Our calculated results of the fluctuations and correlations of conserved charges will be compared with those obtained from very recent lattice calculations performed with an improved staggered fermion action at two values of the lattice cutoff with almost physical up and down quark masses and a physical value for the strange quark mass [28]. On the one hand, our calculations provide insight about what can not be concluded from lattice calculations. For example, whether there is a cusp in the ratio of the quartic to quadratic fluctuations of baryon number χ_4^B/χ_2^B , which is a valuable probe of the deconfinement and chiral dynamics, at the critical temperature can not yet be answered by lattice simulations, because of the larger errors in the calculations, but our calculations indeed find a pronounced cusp in this ratio χ_4^B/χ_2^B at the critical temperature. Furthermore, our calculations give physical interpretation of the lattice data. On the other hand, comparing our calculated results with those obtained in lattice calculations, it allows us to test the validity of the 2+1 flavor PNJL model, and then provide the right direction for improving this effective model.

The paper is organized as follows. In Sec. II we simply review the formalism of the 2+1 flavor PNJL model. In Sec. III we introduce the fluctuations and correlations of conserved charges. In Sec. IV we give our calculated results of fluctuations of light quarks (up and down quarks) and strange quarks. In Sec. V we give our calculated results of fluctuations and correlations of conserved charges, and compare them with those obtained in lattice calculations. In Sec. VI we present our summary and conclusions.

II. 2+1 FLAVOR PNJL MODEL

In this work, we employ the 2+1 flavor Polyakov-loop improved NJL model which has been discussed in details in our previous work [38], and the Lagrangian density for the 2+1

flavor PNJL model is given as

$$\begin{aligned} \mathcal{L}_{PNJL} = & \bar{\psi} (i\gamma_\mu D^\mu + \gamma_0 \hat{\mu} - \hat{m}_0) \psi + G \sum_{a=0}^8 \left[(\bar{\psi} \tau_a \psi)^2 + (\bar{\psi} i\gamma_5 \tau_a \psi)^2 \right] \\ & - K \left[\det_f (\bar{\psi} (1 + \gamma_5) \psi) + \det_f (\bar{\psi} (1 - \gamma_5) \psi) \right] - \mathcal{U}(\Phi, \Phi^*, T), \end{aligned} \quad (1)$$

where $\psi = (\psi_u, \psi_d, \psi_s)^T$ is the three-flavor quark field,

$$D^\mu = \partial^\mu - iA^\mu \quad \text{with} \quad A^\mu = \delta_0^\mu A^0, \quad A^0 = g\mathcal{A}_a^0 \frac{\lambda_a}{2} = -iA_4. \quad (2)$$

λ_a are the Gell-Mann matrices in color space and the gauge coupling g is combined with the SU(3) gauge field $\mathcal{A}_a^\mu(x)$ to define $A^\mu(x)$ for convenience. $\hat{m}_0 = \text{diag}(m_0^u, m_0^d, m_0^s)$ is the three-flavor current quark mass matrix. Throughout this work, we take $m_0^u = m_0^d \equiv m_0^l$, while keep m_0^s being larger than m_0^l , which breaks the $SU(3)_f$ symmetry. The quark chemical potentials are contained in the matrix $\hat{\mu} = \text{diag}(\mu_u, \mu_d, \mu_s)$, and they can also be expressed in terms of chemical potentials for baryon number (μ_B), electric charge (μ_Q), and strangeness (μ_S):

$$\mu_u = \frac{1}{3}\mu_B + \frac{2}{3}\mu_Q, \quad \mu_d = \frac{1}{3}\mu_B - \frac{1}{3}\mu_Q, \quad \text{and} \quad \mu_s = \frac{1}{3}\mu_B - \frac{1}{3}\mu_Q - \mu_S. \quad (3)$$

In the above PNJL Lagrangian, $\mathcal{U}(\Phi, \Phi^*, T)$ is the Polyakov-loop effective potential, which is expressed in terms of the traced Polyakov-loop $\Phi = (\text{Tr}_c L)/N_c$ and its conjugate $\Phi^* = (\text{Tr}_c L^\dagger)/N_c$ with the Polyakov-loop L being a matrix in color space given explicitly by

$$L(\vec{x}) = \mathcal{P} \exp \left[i \int_0^\beta d\tau A_4(\vec{x}, \tau) \right] = \exp [i\beta A_4], \quad (4)$$

with $\beta = 1/T$ being the inverse of temperature and $A_4 = iA^0$.

In our work, we use the Polyakov-loop effective potential which is a polynomial in Φ and Φ^* [42], given by

$$\frac{\mathcal{U}(\Phi, \Phi^*, T)}{T^4} = -\frac{b_2(T)}{2} \Phi^* \Phi - \frac{b_3}{6} (\Phi^3 + \Phi^{*3}) + \frac{b_4}{4} (\Phi^* \Phi)^2, \quad (5)$$

with

$$b_2(T) = a_0 + a_1 \left(\frac{T_0}{T} \right) + a_2 \left(\frac{T_0}{T} \right)^2 + a_3 \left(\frac{T_0}{T} \right)^3. \quad (6)$$

Parameters in the effective potential are fitted to reproduce the thermodynamical behavior of the pure gauge QCD obtained from the lattice simulations, and their values are given in Table I. The parameter T_0 is the critical temperature for the deconfinement phase transition

TABLE I: Parameters for the Polyakov-loop effective potential \mathcal{U}

| a_0 | a_1 | a_2 | a_3 | b_3 | b_4 |
|-------|-------|-------|-------|-------|-------|
| 6.75 | -1.95 | 2.625 | -7.44 | 0.75 | 7.5 |

to take place in the pure-gauge QCD and T_0 is chosen to be 270 MeV according to the lattice calculations.

In the mean field approximation, the thermodynamical potential density for the 2+1 flavor quark system is given by

$$\begin{aligned}
 \Omega = & -2N_c \sum_{f=u,d,s} \int \frac{d^3p}{(2\pi)^3} \left\{ E_p^f \theta(\Lambda^2 - p^2) \right. \\
 & + \frac{T}{3} \ln \left[1 + 3\Phi^* e^{-(E_p^f - \mu_f)/T} + 3\Phi e^{-2(E_p^f - \mu_f)/T} + e^{-3(E_p^f - \mu_f)/T} \right] \\
 & + \frac{T}{3} \ln \left[1 + 3\Phi e^{-(E_p^f + \mu_f)/T} + 3\Phi^* e^{-2(E_p^f + \mu_f)/T} + e^{-3(E_p^f + \mu_f)/T} \right] \Big\} \\
 & + 2G(\phi_u^2 + \phi_d^2 + \phi_s^2) - 4K\phi_u\phi_d\phi_s + \mathcal{U}(\Phi, \Phi^*, T).
 \end{aligned} \tag{7}$$

where ϕ_i ($i = u, d, s$) is the chiral condensate of quarks with flavor i , and we have the energy-momentum dispersion relation $E_p^i = \sqrt{p^2 + M_i^2}$ for its corresponding quasiparticle, with the constituent mass for the quark of flavor i being

$$M_i = m_0^i - 4G\phi_i + 2K\phi_j\phi_k. \tag{8}$$

Minimizing the thermodynamical potential in Eq. (7) with respect to ϕ_u , ϕ_d , ϕ_s , Φ , and Φ^* , we obtain a set of equations of motion

$$\frac{\partial \Omega}{\partial \phi_u} = 0, \quad \frac{\partial \Omega}{\partial \phi_d} = 0, \quad \frac{\partial \Omega}{\partial \phi_s} = 0, \quad \frac{\partial \Omega}{\partial \Phi} = 0, \quad \frac{\partial \Omega}{\partial \Phi^*} = 0. \tag{9}$$

Then, this set of equations can be solved as functions of temperature T and three flavor quark chemical potentials μ_u , μ_d , and μ_s or chemical potentials of conserved charges μ_B , μ_Q , and μ_S .

III. FLUCTUATIONS AND CORRELATIONS

Following the procedure in lattice calculations [28], we focus on the derivatives of the pressure ($P = -\Omega$) of the thermodynamical system with respect to the chemical potentials

corresponding to the conserved charge: baryon number, electric charge, and strangeness, i.e.

$$\chi_{ijk}^{BQS} = \frac{\partial^{i+j+k}(P/T^4)}{\partial(\mu_B/T)^i \partial(\mu_Q/T)^j \partial(\mu_S/T)^k} \Big|_{\mu_B, Q, S=0}, \quad (10)$$

which are evaluated at $\mu_{B,Q,S} = 0$. The χ 's in Eq. (10) are in fact the generalized susceptibilities and they are related with the moments of charge fluctuations, i.e. $\delta N_X \equiv N_X - \langle N_X \rangle$ ($X = B, Q, S$) and the correlations among conserved charges. Taking the quadratic, quartic and the 6th order charge fluctuations for example, we have

$$\chi_2^X = \frac{1}{VT^3} \langle \delta N_X^2 \rangle, \quad (11)$$

$$\chi_4^X = \frac{1}{VT^3} \left(\langle \delta N_X^4 \rangle - 3 \langle \delta N_X^2 \rangle^2 \right), \quad (12)$$

$$\chi_6^X = \frac{1}{VT^3} \left(\langle \delta N_X^6 \rangle - 15 \langle \delta N_X^4 \rangle \langle \delta N_X^2 \rangle - 10 \langle \delta N_X^3 \rangle^2 + 30 \langle \delta N_X^2 \rangle^3 \right). \quad (13)$$

And the correlations among two conserved charges are

$$\chi_{11}^{XY} = \frac{1}{VT^3} \langle N_X N_Y \rangle. \quad (14)$$

It should be noted that the fluctuations and correlations of conserved charges, i.e. the generalized susceptibilities in Eq. (10) are nonvanishing only when $i + j + k$ is even at vanishing chemical potentials $\mu_{B,Q,S} = 0$.

In this work we use the method of Taylor expansion to compute the fluctuations and correlations of conserved charges in the PNJL model. Before our numerical calculations, we should determine the five parameters in the quark sector of the model. Values of the five parameters used usually in the literatures are obtained in Ref. [48], which are $m_0^l = 5.5$ MeV, $m_0^s = 140.7$ MeV, $GA^2 = 1.835$, $K\Lambda^5 = 12.36$ and $\Lambda = 602.3$ MeV. They are fixed by fitting $m_\pi = 135.0$ MeV, $m_K = 497.7$ MeV, $m_{\eta'} = 957.8$ MeV and $f_\pi = 92.4$ MeV. For convenience to compare our calculations with the recent lattice simulations in which the strange quark mass has been tuned close to its physical value and the light quark masses have been chosen to be one tenth of the strange quark mass [28], we employ the values of the five parameters given above except with $m_0^l = 14.0$ MeV, which is consistent with the lattice calculations.

IV. FLUCTUATIONS OF LIGHT QUARKS AND STRANGE QUARKS

In order to understand the behavior of the fluctuations of conserved charges better, we will study the fluctuations of light quarks and strange quarks in this section. In Fig. 1

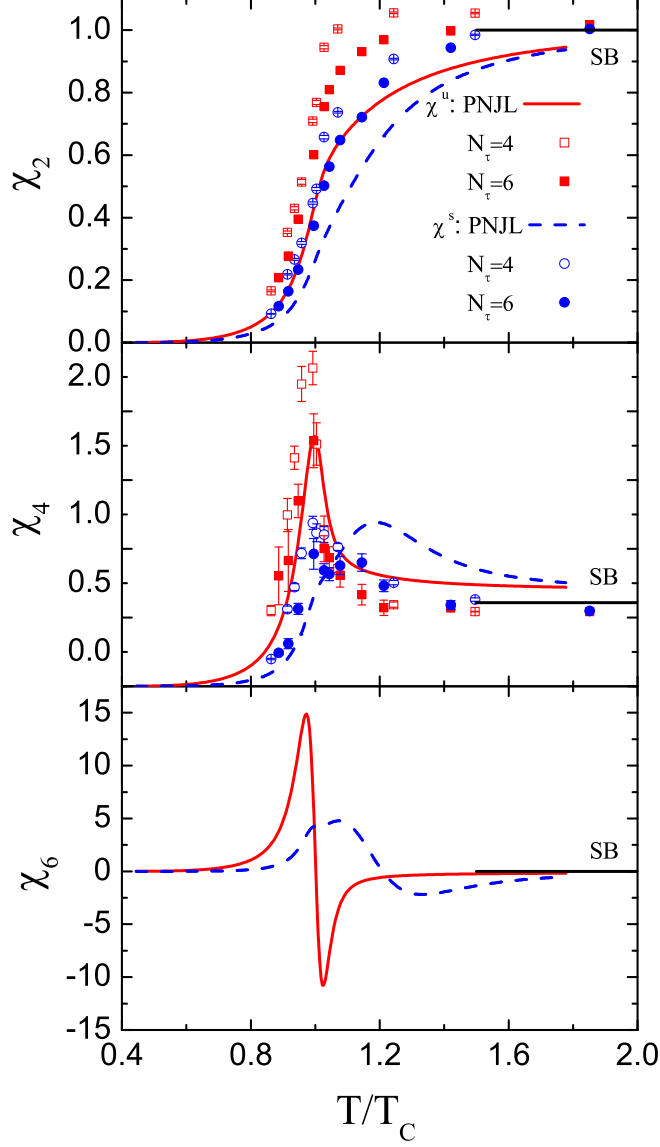


FIG. 1: (color online). Quadratic (top), quartic (middle) and the 6th order (bottom) fluctuations of light quarks (here we denote them with χ^u) and strange quarks as functions of the temperature (in unit of the critical temperature T_C) calculated in the PNJL model with $m_0^l = 14.0$ MeV and $m_0^s = 140.7$ MeV. We also show the results of the quadratic and quartic fluctuations obtained from calculations on $16^3 \times 4$ and $24^3 \times 6$ lattices in Ref. [28]. Here SB denotes the corresponding limit value of Stefan-Boltzmann ideal gas.

we show the quadratic, quartic and the 6th order fluctuations of light and strange quarks versus temperature. We find that the pseudo-critical temperature for the chiral restoration phase transition is 225 MeV and that for the deconfinement phase transition is 221 MeV

at vanishing chemical potential in the PNJL model with $m_0^l = 14.0$ MeV, $m_0^s = 140.7$ MeV and other parameters given above. More detailed discussions about the different phase transitions can be found in Ref [38]. Since these two critical temperatures for the two different kinds of phase transitions are almost same, we just need one value of temperature to locate the two phase transitions and here we choose $T_C = 225$ MeV which is used as unit in Fig. 1. Furthermore, we also present the results of the quadratic and quartic fluctuations obtained from calculations on $16^3 \times 4$ and $24^3 \times 6$ lattices in Ref [28] in Fig. 1. From the top panel of Fig. 1 ones can find that the quadratic fluctuations calculated in the PNJL model increase monotonously with the increase of the temperature, and the fluctuations of the heavier strange quarks are suppressed relative to those of the light quarks. These features are consistent with the lattice calculations (also the lattice simulations in Ref. [20]). Comparing our results with those from lattice calculations, we find that the quadratic fluctuations calculated in the PNJL model are relatively smaller than those calculated in the lattice simulations. And we also find that the quadratic fluctuations calculated in the lattice simulations rapidly approach the Stefan-Boltzmann ideal massless gas value, i.e. $\chi_2^{SB} = 1$ when the temperature is above the critical temperature, while the quadratic fluctuations calculated in the PNJL model approach the Stefan-Boltzmann value more slowly, which is because the current quark mass effect is obvious at high temperature in the PNJL model.

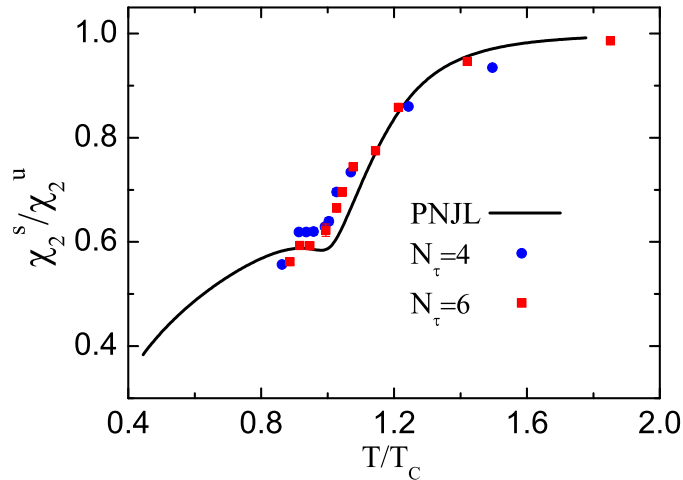


FIG. 2: (color online). Ratio of s and u quark quadratic fluctuations as function of the temperature calculated in the PNJL model with $m_0^l = 14.0$ MeV and $m_0^s = 140.7$ MeV and in simulations on $16^3 \times 4$ and $24^3 \times 6$ lattices in Ref. [28].

In Fig. 2 we show the ratio of strange and light quark quadratic fluctuations as function of the temperature. Our calculations clearly indicate that the quadratic fluctuations of strange quarks are smaller than those of light quarks at low temperature, which are consistent with the lattice calculations. Furthermore, we find a plateau at the critical temperature in the curve of χ_2^s/χ_2^u versus temperature in our calculations, as the solid line shows in Fig. 2. This plateau can also be found in the lattice data.

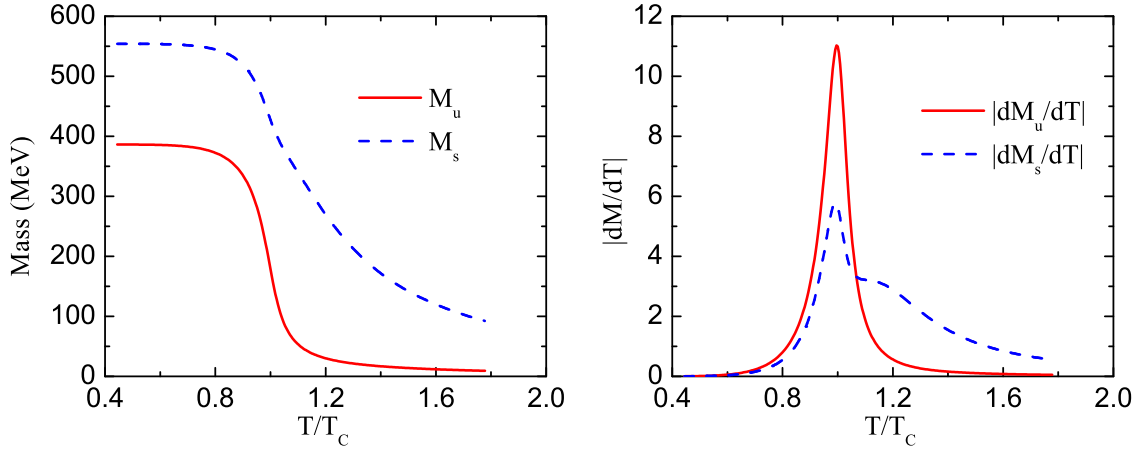


FIG. 3: (color online). Left panel: constituent masses of light quarks and strange quarks as functions of the temperature at vanishing chemical potentials in the PNJL model with $m_0^l = 14.0$ MeV and $m_0^s = 140.7$ MeV. Right panel: corresponding derivatives of constituent masses of light quarks and strange quarks with respect to the temperature, and here we use the absolute values of the derivatives.

As for the quartic fluctuations, we find that the fluctuations of light quarks calculated in the PNJL model is consistent with those obtained from the lattice calculations, especially during the phase transition where a sharp peak appears at T_C . Furthermore, lattice calculations show that there is a relatively lower peak at T_C as well for the quartic fluctuations of strange quarks, while our calculations indicate that the peak corresponding to the strange quarks is shifted to about $1.2T_C$ and becomes broader and lower. To explore the reason for the difference between our and lattice calculations, we show the constituent masses of light quarks and strange quarks, and also their derivatives with respect to temperature as functions of the temperature in Fig. 3. One can find that the constituent mass of light quarks rapidly decreases to their current quark mass at T_C , which corresponds to a sharp

peak of the curve $|dM_u/dT|$ at the critical temperature as the right panel of Fig. 3 shows. However, for the strange quarks, the constituent mass still decreases slowly beyond the critical temperature, which results in a plateau of the curve $|dM_s/dT|$ at about $1.2T_C$. That is the reason why the quartic fluctuations of strange quarks present a broad peak at $1.2T_C$ in the PNJL model. In the bottom panel of Fig. 1 we show the 6th order fluctuations of light quarks and strange quarks. One can find that the 6th order fluctuations of light quarks oscillate violently at T_C , while those of strange quarks oscillate mildly at relatively larger temperature.

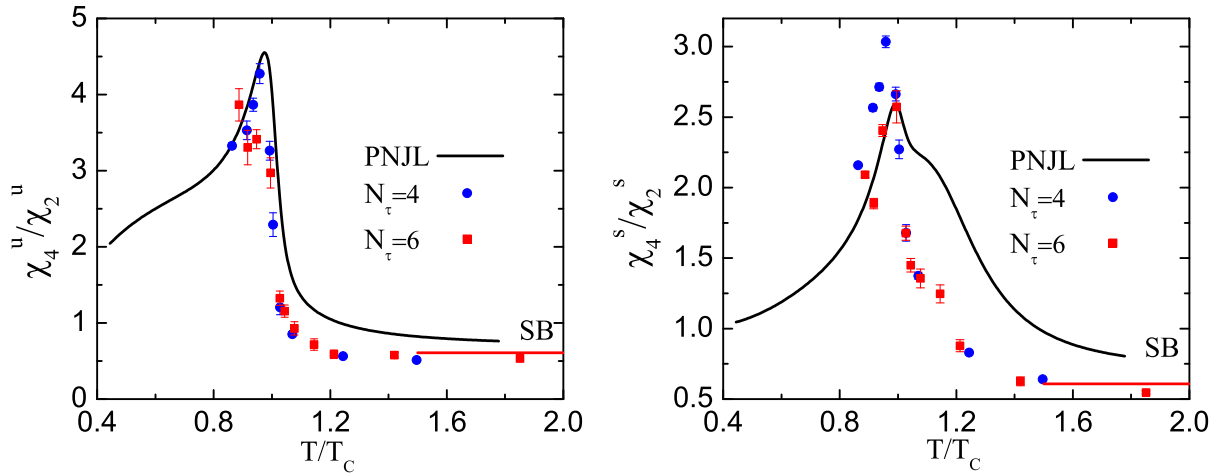


FIG. 4: (color online). Ratio of the quartic to quadratic fluctuations for light quarks (left panel) and strange quarks (right panel) as functions of the temperature calculated in the PNJL model with $m_0^l = 14.0$ MeV and $m_0^s = 140.7$ MeV, which are also compared with those obtained from calculations on $16^3 \times 4$ and $24^3 \times 6$ lattices in Ref. [28].

In the following we pay more attentions to the ratio of the quartic to quadratic fluctuations of the quark number, since this ratio is believed to be a valuable probe of the deconfinement and chiral phase transitions [24–26, 36]. Fig. 4 shows this ratio for the light quarks and strange quarks calculated in our PNJL model, and we also show the corresponding results obtained in the lattice simulations for comparisons. Our calculations indicate that, for both light quarks and strange quarks, the ratio of the quartic to quadratic fluctuations of the quark number increases with the temperature below the critical temperature, while decreases when the temperature is above the critical one. So there is a peak in the curve of the ratio versus temperature at the critical temperature for both light quarks and strange quarks.

These features are consistent with those obtained in the lattice calculations. Comparing the two panels of Fig. 4 we find that the consistency between our calculations and the lattice simulations for the light quarks is better than that for the strange quarks, which can be expected, since for the quartic fluctuations of strange quarks the difference between the PNJL model and the lattice simulations is quite larger than that for the light quarks, as shown in the middle panel of Fig. 1.

Next, we discuss the ratio of the quartic to quadratic fluctuations when the temperature is away from the phase transition temperature. As the temperature is high, especially when the temperature is quite above the critical temperature, the system can be approximated as noninteracting massless gases. That is the Stefan-Boltzmann limit, and in this limit the pressure of the quarks and antiquarks can be easily obtained as

$$\frac{P}{T^4} = \sum_{f=u,d,s} N_c \left[\frac{7\pi^2}{180} + \frac{1}{6} \left(\frac{\mu_f}{T} \right)^2 + \frac{1}{12\pi^2} \left(\frac{\mu_f}{T} \right)^4 \right]. \quad (15)$$

So in the Stefan-Boltzmann limit, $\chi_4/\chi_2 = 6/\pi^2$.

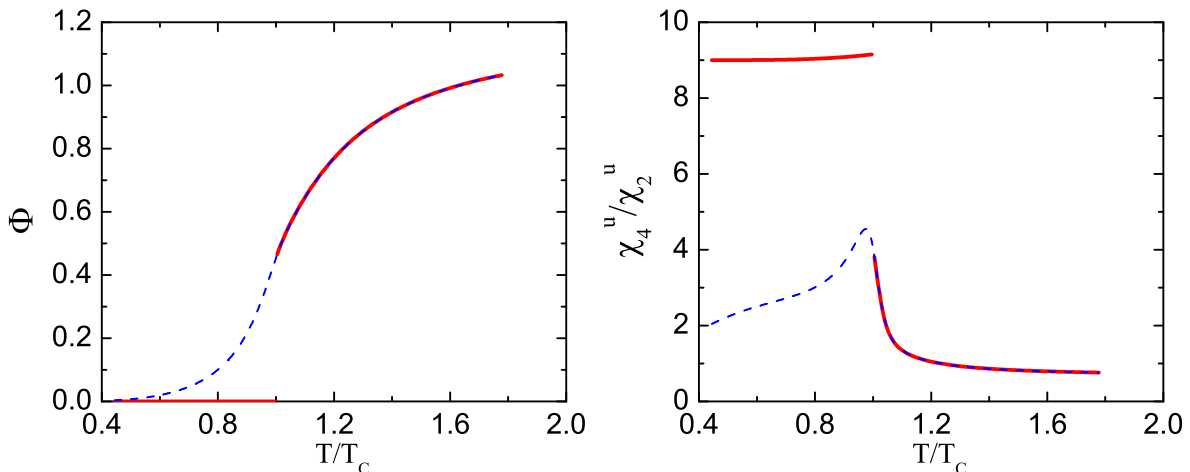


FIG. 5: (color online). Left panel: Polyakov-loop versus temperature in two cases at vanishing chemical potentials in the PNJL model with $m_0^l = 14.0$ MeV and $m_0^s = 140.7$ MeV ($\Phi^* = \Phi$ at vanishing chemical potentials). The blue dashed line corresponds to our full calculations, and the red solid line to the calculations in which Φ and Φ^* are set to be zero artificially when the temperature is below the critical temperature. Right panel: ratio of the quartic to quadratic fluctuations for light quarks corresponding to the two cases. Therefore, the blue dashed line represents the same results which have been shown in the left panel of Fig. 4.

On the contrary, when the temperature is below the critical temperature, the constituent masses of quarks are much larger than their current masses as the left panel of Fig. 3 shows. Furthermore, quarks tend to be combined to form colorless hadrons, which is the color confinement. In the PNJL model, we can not include the degrees of freedom of hadrons, but this effective model embodies the confinement effect by suppressing the excitations of the one and two quark states and only permitting those of three quark states [38]. In details, when the temperature is much lower than the critical temperature, the Polyakov-loop and its conjugate $\Phi, \Phi^* \rightarrow 0$, and then most contributions to the pressure of the thermodynamical system come from the three quark states. Since the constituent masses of quarks are much larger than the temperature, we can use the Boltzmann approximation [36], and the pressure is

$$\frac{P}{T^4} \simeq \sum_{f=u,d,s} N_c \frac{2}{81\pi^2} \left(\frac{3m_f}{T}\right)^2 K_2\left(\frac{3m_f}{T}\right) \cosh\left(\frac{3\mu_f}{T}\right). \quad (16)$$

Where K_2 is a Bessel function. Then we can easily obtain $\chi_4/\chi_2 = 9$. It should be emphasized that, since the temperature driven deconfinement transition is not a strict phase transition but a continuous crossover [21, 22], the Polyakov-loop Φ (or Φ^*) is not vanishing when the temperature is below the critical one as the blue dashed line shows in the left panel of Fig. 5. Assuming $\Phi = \Phi^* = 1$ even when $T < T_C$, we obtain

$$\frac{P}{T^4} \simeq \sum_{f=u,d,s} N_c \frac{2}{\pi^2} \left(\frac{m_f}{T}\right)^2 K_2\left(\frac{m_f}{T}\right) \cosh\left(\frac{\mu_f}{T}\right). \quad (17)$$

Then we have $\chi_4/\chi_2 = 1$ in this situation. Since Φ (or Φ^*) is between 0 and 1 at low temperature as we have mentioned above, we expect χ_4/χ_2 to be between 1 and 9 when $T < T_C$. This expectation is verified in our numerical calculations as shown in Fig. 4. For comparison, we set Φ and Φ^* to be zero artificially when the temperature is below the critical temperature as the red solid line shows in the left panel of Fig. 5, then we calculate the corresponding χ_4^u/χ_2^u . The results are shown in the right panel of Fig. 5, which clearly indicates that χ_4^u/χ_2^u approaches 9 when $T < T_C$. One can easily find that the ratio of the quartic to quadratic fluctuations calculated in the case in which the Polyakov-loop is set to be zero artificially is not consistent with the lattice calculations.

So far, we have found that the calculations in the PNJL model for the light quark fluctuations are consistent with those in the lattice simulations, while for the strange quark fluctuations, since the current mass of the strange quarks is large, there are rela-

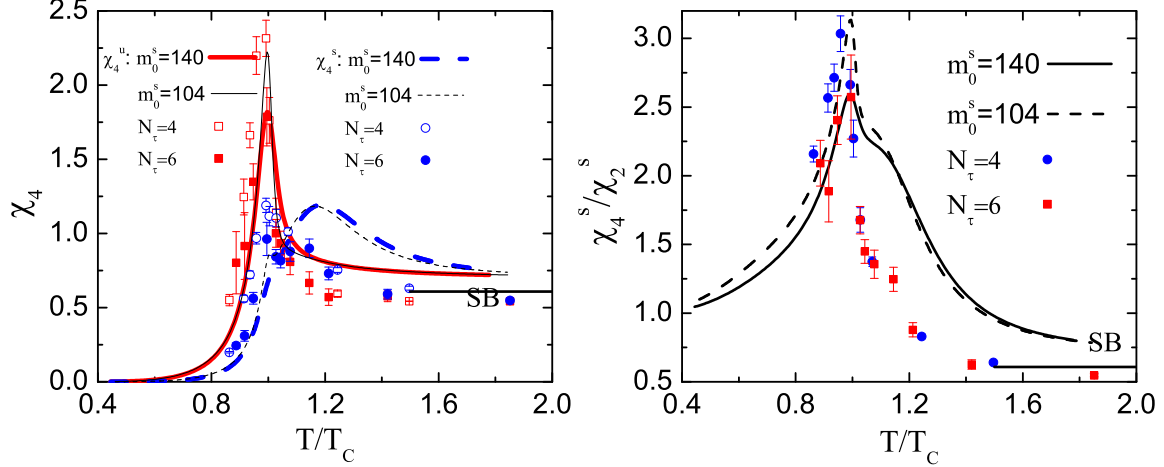


FIG. 6: (color online). Left panel: quartic fluctuations of light quarks and strange quarks as functions of the temperature in the PNJL model with different quark current masses, one with $m_0^l = 14.0$ MeV and $m_0^s = 140.7$ MeV (same as our previous calculations) and the other with $m_0^l = 3.79$ MeV and $m_0^s = 104$ MeV. In the same way, the corresponding results obtained in QCD simulations on $16^3 \times 4$ and $24^3 \times 6$ lattices in Ref. [28] are also presented. Right panel: ratio of the quartic to quadratic fluctuations for strange quarks as functions of the temperature in the PNJL model with the two sets of current quark masses.

tively larger differences between the results in the PNJL model and those in lattice calculations. Considering the value of the strange quark current mass used in the PNJL model ($m_0^s = 140.7$ MeV) is relatively larger than the middle value 104 MeV given by the PDG2008 ($m_0^s = 104_{-34}^{+26}$ MeV [49]), we set $m_0^s = 104$ MeV and $m_0^l = 3.79$ MeV in the PNJL model and leave other parameters unchanged (here $m_0^l = 3.79$ MeV is the middle value of the average mass of up and down quarks given by the PDG2008 ($\overline{m} = (m_u + m_d)/2 = 3.79_{-1.29}^{+1.21}$ MeV [49])). Then we repeat the calculations above. Fig. 6 shows the quartic fluctuations of light quarks and strange quarks, and the ratio of the quartic to quadratic fluctuations for strange quarks with the two sets of current quark masses. We find that the height of the peak in the quartic fluctuations of light quarks at the critical temperature is enhanced due to the reduction of light quark current mass, and with the decrease of the strange quark mass, the broad peak of the curve χ_4^s move a little to low temperature. However, there are also differences between the PNJL model with $m_0^s = 104$ MeV and the lattice simulations for the χ_4^s and χ_4^s/χ_2^s .

V. FLUCTUATIONS AND CORRELATIONS OF CONSERVED CHARGES

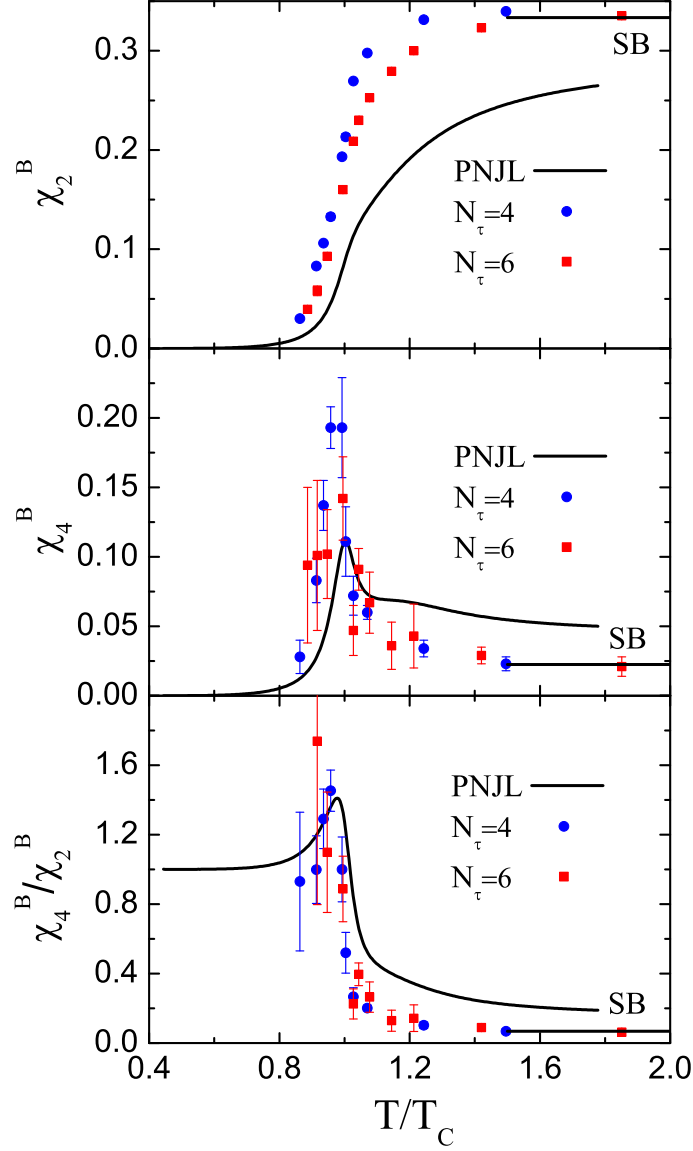


FIG. 7: (color online). Quadratic (top), quartic (middle) fluctuations of baryon number, and their ratio (bottom) as functions of the temperature calculated in the PNJL model with $m_0^l = 14.0$ MeV and $m_0^s = 140.7$ MeV. The corresponding results obtained from calculations on $16^3 \times 4$ and $24^3 \times 6$ lattices in Ref. [28] are also presented.

We have discussed the fluctuations of light quarks and strange quarks in details above. In the following, we will focus on the fluctuations of baryon number, electric charge, and strangeness.

Fig. 7 shows the quadratic and quartic fluctuations of the baryon number, and their ratio

versus temperature calculated in the PNJL model and in the lattice simulations. Same as the fluctuations of light quarks and strange quarks, We find that the quadratic fluctuations of baryon number increase monotonically with the temperature, while the quartic fluctuations develop a cusp at the critical temperature and decrease with increase of the temperature when $T > T_C$. As a matter of fact, the singular behavior of the baryon number fluctuations is expected to be controlled by the universal $O(4)$ symmetry group at vanishing chemical potential and vanishing light quark mass [31]. And the baryon number fluctuations are expected to scale like [28],

$$\chi_{2n}^B \sim \left| \frac{T - T_C}{T_C} \right|^{2-n-\alpha} \quad (18)$$

with $\alpha \simeq -0.25$. As Eq. (18) shows, with the increase of the order, the singular properties of the baryon number fluctuations become more and more prominent, which are confirmed both in the calculations of the PNJL model and in the lattice simulations. Comparing the results obtained in the PNJL model and those in lattice calculations, we find that our results are consistent with the lattice results qualitatively, but the differences in quantities between the two results still exist, especially at high temperature. The reason for these differences has been mentioned above, i.e. when the temperature is high, the current quark mass effect becomes more and more important.

The bottom panel of Fig. 7 shows the ratio of the quartic to quadratic fluctuations of the baryon number. We find that this ratio approaches 1 at low temperature, which is consistent with the lattice results as well as the calculations in the hadron resonance gas model [28, 50]. An interesting thing is that we find a pronounced cusp in the ratio χ_4^B/χ_2^B at the critical temperature in our calculations. However, whether the cusp exists in the lattice results is not clear, because the errors are very large at low temperature as the figure shows. We have emphasized that answering the question whether there is a cusp in the ratio of the quartic to quadratic fluctuations is very important, because this ratio is a valuable probe of the deconfinement and chiral phase transitions and have received lots of attentions recent years [27, 36]. Our calculations indicate that the cusp in the ratio χ_4^B/χ_2^B is prominent even with physical strange quark mass $m_0^s = 140.7$ MeV and relatively larger (comparing with the physical value) light quark mass $m_0^l = 14.0$ MeV.

In Fig. 8, we show the quadratic, quartic and the 6th order fluctuations of electric charge versus temperature obtained in our calculations and lattice simulations. Once more, we find that the electric charge quadratic fluctuations increase monotonically with the temperature

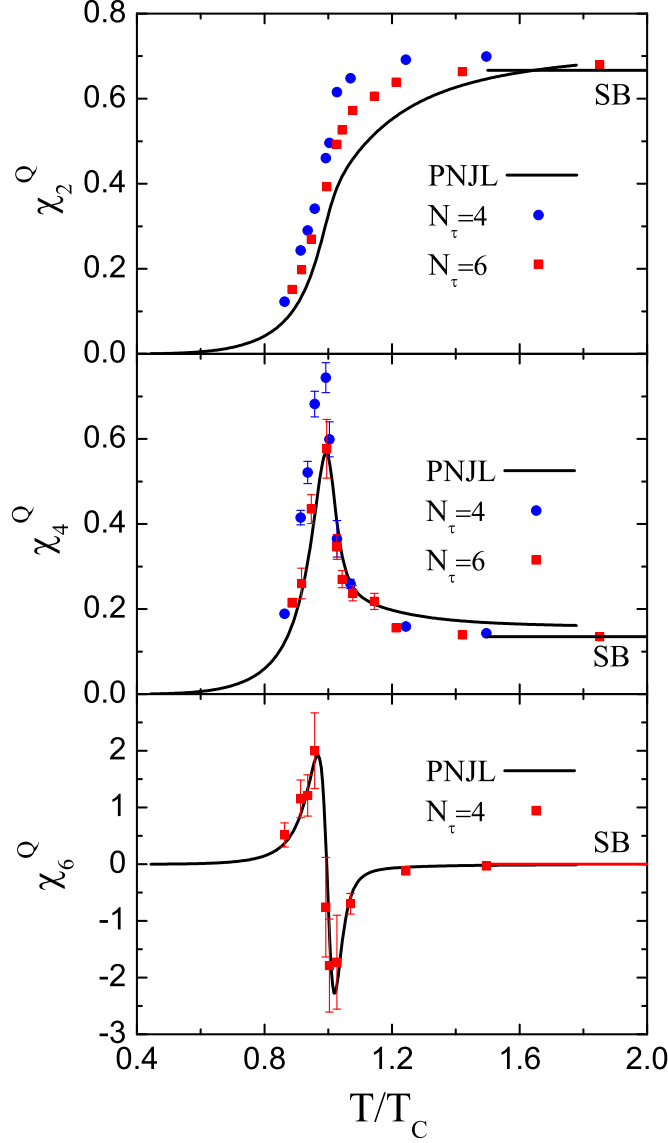


FIG. 8: (color online). Quadratic (top), quartic (middle) and the 6th order (bottom) fluctuations of electric charge as functions of the temperature obtained in the PNJL model with $m_0^l = 14.0$ MeV and $m_0^s = 140.7$ MeV and in the QCD simulations on $16^3 \times 4$ and $24^3 \times 6$ lattices in Ref. [28].

and the quartic fluctuations of the electric charge present a prominent cusp at the critical temperature. As for the 6th order fluctuations of electric charge, we find a pronounced oscillation happening during the deconfinement and chiral phase transitions. χ_6^Q is vanishing when the temperature is below about $0.8T_C$, and with the temperature being increased beyond $0.8T_C$, the 6th order fluctuations increase rapidly. When the temperature is near T_C , χ_6^Q changes from a positive value to a negative one abruptly. Then, χ_6^Q increases with

the temperature and approaches the Stefan-Boltzmann value ($\chi_6^{Q,SB} = 0$) from below. From the bottom panel of Fig. 8, One can find that the 6th order fluctuations of electric charge are almost odd functions with respect to $T - T_C$. Comparing Fig. 8 with Fig. 7, we find that the fluctuations of electric charge calculated in the PNJL model are better consistent with those obtained in lattice calculations than the fluctuations of the baryon number. This is because more contributions to the electric charge fluctuations come from the light quarks, since the absolute value of the electric charge of u quarks $2/3$ is larger than that of s quarks $1/3$.

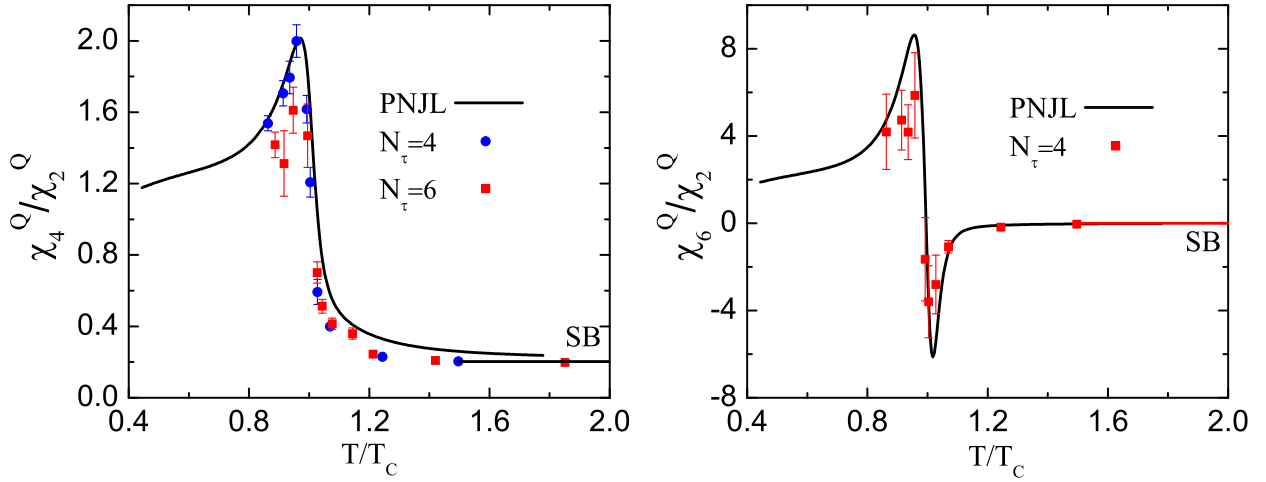


FIG. 9: (color online). Left panel: Ratio of the quartic to quadratic electric charge fluctuations versus temperature obtained in the PNJL model with $m_0^l = 14.0$ MeV and $m_0^s = 140.7$ MeV and in the QCD simulations on $16^3 \times 4$ and $24^3 \times 6$ lattices in Ref [28]. Right panel: Ratio of the 6th to 2nd order fluctuations of electric charge versus temperature calculated in the PNJL model with $m_0^l = 14.0$ MeV and $m_0^s = 140.7$ MeV and in the QCD simulations on $16^3 \times 4$ lattices in Ref. [28].

In Fig. 9, we show the ratios of the 4th to 2nd order and the 6th to 2nd order fluctuations of electric charge as functions of the temperature obtained in the PNJL model and the lattice simulations. One can find that the results given by the PNJL model are well consistent with those obtained in the lattice simulations. Comparing χ_4^Q/χ_2^Q with χ_4^B/χ_2^B in the bottom panel of Fig. 7, we find there is a prominent cusp at the critical temperature in the curve of χ_4^Q/χ_2^Q as same as that in the curve of χ_4^B/χ_2^B . However, different from χ_4^B/χ_2^B , at low temperature χ_4^Q/χ_2^Q is larger than unity and is a raising function of the temperature, since it is expected that at low temperature quartic fluctuations of electric charge are enhanced

relative to the quadratic fluctuations [28]. As for the ratio χ_6^Q/χ_2^Q , we find it oscillates violently at the phase transition temperature.

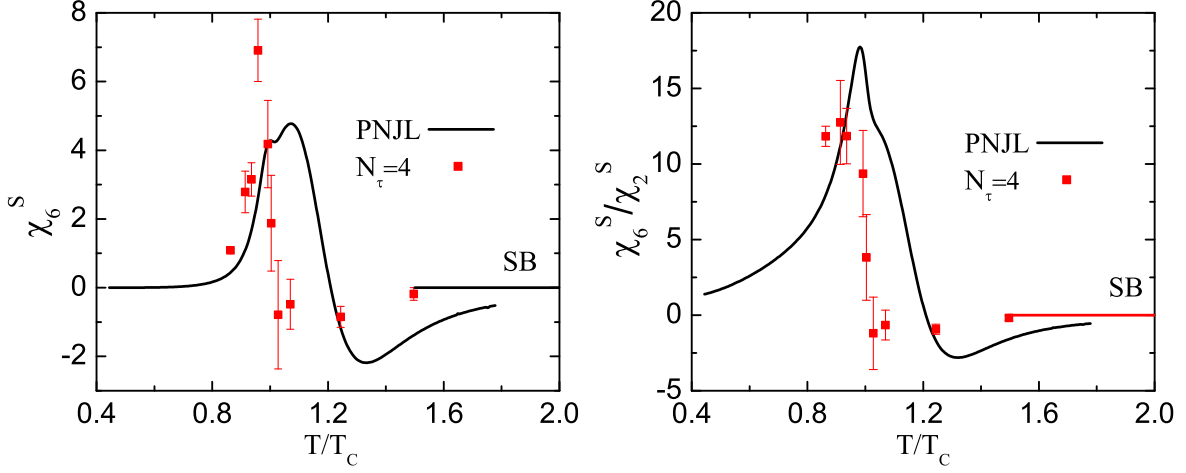


FIG. 10: (color online). The 6th order fluctuations of strangeness (left panel) and the ratio χ_6^s/χ_2^s (right panel) as functions of the temperature calculated in the PNJL model with $m_0^l = 14.0$ MeV and $m_0^s = 140.7$ MeV and in the QCD simulations on $16^3 \times 4$ lattices in Ref. [28].

We have discussed the quadratic and quartic fluctuations of the strange quarks in details above. It is easily verified that the fluctuations of strange quarks are identical to those of strangeness. Therefore, we will focus on the 6th order fluctuations of strangeness in the following. Fig. 10 shows the 6th order fluctuations of strangeness and the ratio χ_6^s/χ_2^s as functions of the temperature calculated in the PNJL model, which are also compared with the QCD simulations on $16^3 \times 4$ lattices in Ref [28]. We find that χ_6^s and χ_6^s/χ_2^s obtained in the PNJL model are qualitatively consistent with those obtained in lattice simulations, i.e. χ_6^s and χ_6^s/χ_2^s oscillate during the deconfinement and chiral phase transitions. However, there are some quantitative differences between these two approaches: the temperature where χ_6^s and χ_6^s/χ_2^s vanish during the oscillation in the PNJL model is shifted from T_C to about $1.2T_C$ with respect to the results in the lattice simulations. Similar phenomena have been found in the calculations of χ_4^s and χ_4^s/χ_2^s above in Fig. 6, since much larger current mass of the strange quarks results in that the chiral restoration phase transition for the strange quark sector occurs at relative larger temperature than that for the light quark sector as Fig. 3 shows.

In Fig. 11, we show correlations among conserved charges, in more details, including

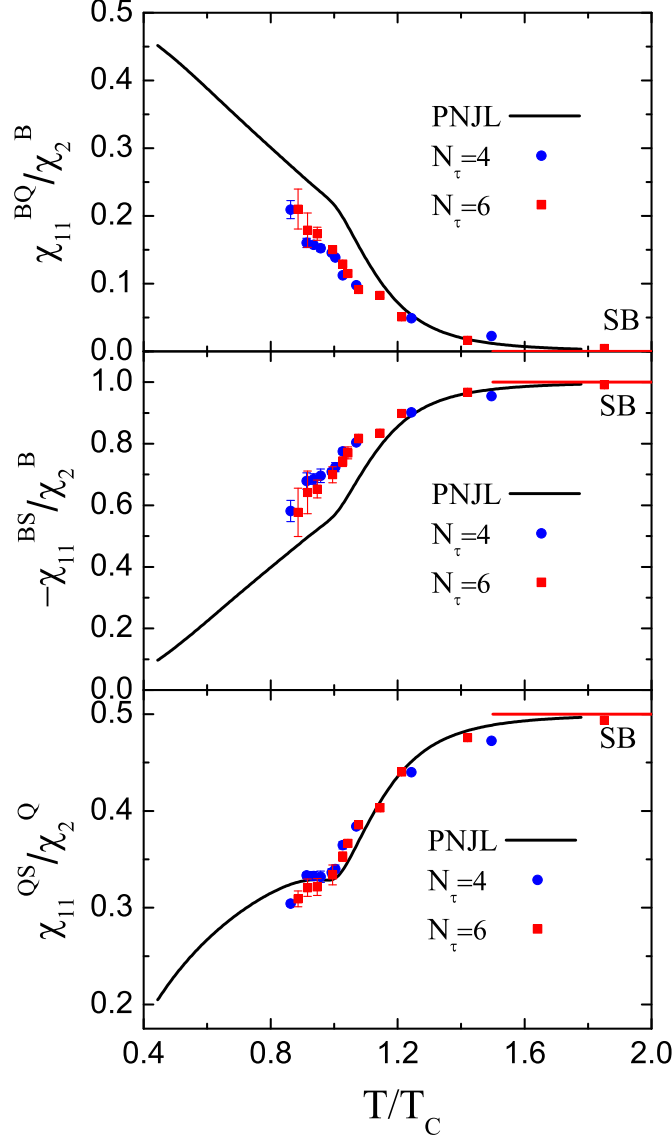


FIG. 11: (color online). Correlations of baryon number and electric charge normalized to quadratic fluctuations of baryon number (top), baryon number and strangeness to quadratic fluctuations of baryon number (middle), and electric charge and strangeness to quadratic fluctuations of electric charge (bottom) as functions of the temperature obtained in the PNJL model with $m_0^l = 14.0$ MeV and $m_0^s = 140.7$ MeV and in the QCD simulations on $16^3 \times 4$ and $24^3 \times 6$ lattices in Ref. [28].

the correlations of baryon number and electric charge, baryon number and strangeness and those of electric charge and strangeness. The former two correlations are normalized to the quadratic fluctuations of baryon number and the last one is to quadratic fluctuations of electric charge. One can find that χ_{11}^{BQ}/χ_2^B calculated in the PNJL model decreases with the

increase of the temperature, which agrees with the calculations in lattice simulations. When the temperature is about $1.5T_C$, this ratio approaches zero, the limit value of noninteracting massless quark gas, since the sum of electric charges of light quarks and strange quarks vanishes in this limit. One can also find that our calculated results of χ_{11}^{BQ}/χ_2^B are a little larger than those of lattice calculations at the critical temperature, but well consistent with the lattice results at high temperature. The correlation between baryon number and strangeness has been thought as a useful diagnostic of strongly interacting matter, which can be extracted not only theoretically from lattice QCD and effective model calculations but also experimentally from event-by-event fluctuations [35]. We find that the correlation of baryon number and strangeness approaches zero at low temperature, since the strange hadrons (here in the PNJL model are the three quark clusters with strange quarks) are much heavier to excite in the thermodynamical system. The ratio $-\chi_{11}^{BS}/\chi_2^B$ calculated in the PNJL model increases with the temperature and approaches the Stefan-Boltzmann value at about $1.5T_C$, which agrees with the lattice QCD simulations. Same as the correlation of baryon number and strangeness, the correlation of strangeness and electric charge is also suppressed at low temperature and the ratio χ_{11}^{QS}/χ_2^Q increase with the temperature. One can find that our calculated results of χ_{11}^{QS}/χ_2^Q are well consistent with those of the lattice simulations. An interesting thing is that both the results given by the two approaches indicate that there is a plateau in the ratio of χ_{11}^{QS}/χ_2^Q at the critical temperature.

VI. SUMMARY AND DISCUSSIONS

In this work, we have studied the fluctuations and correlations of the conserved charges, i.e. the baryon number, electric charge and the strangeness, in the Polyakov–Nambu–Jona-Lasinio (PNJL) model at finite temperature. We have also compared our calculated results with those obtained from the recent lattice calculations performed with an improved staggered fermion action at two values of the lattice cutoff with almost physical up and down quark masses and a physical value for the strange quark mass [28].

In order to study the fluctuations of conserved charges much better, we have calculated the fluctuations of light quarks (up and down quarks) and strange quarks before the calculations for the conserved charges. Our calculations indicate that the quadratic fluctuations of light quarks, strange quarks and conserved charges (including the baryon number, electric charge

and the strangeness) increase from zero at low temperature to their corresponding Stefan-Boltzmann values at high temperature, since particles excited at finite temperature are increased with the increase of temperature; the quartic fluctuations are characterized by an pronounced cusp (the cusp is high and sharp for light quarks and low and broad for strange quarks, but both are prominent) during the deconfinement and chiral phase transitions; the 6th order fluctuations for the quarks and conserved charges oscillate with the occurrence of the phase transitions. These qualitative features shown in our calculations are well consistent with those given by the lattice calculations, which confirms that the effective model (here is the PNJL model) captures the right symmetry of the QCD, i.e. the chiral symmetry group, since different phase transitions are govern by different symmetry groups.

Comparing our calculated results with those obtained in lattice QCD simulations quantitatively, we have found that the fluctuations of light quarks obtained in the PNJL model are well consistent with those calculated in the lattice simulations. However, for the fluctuations of strange quarks, there are discrepancies between these two approaches. In more details, calculations of the PNJL model indicate that the cusp of the quartic fluctuations and the oscillation of the 6th order fluctuations for strange quarks are located at about $1.2T_C$, while they are still located at T_C as same as the light quarks in the lattice calculations in Ref. [28]. The reason for this discrepancy is that the pseudo-critical temperature of the chiral restoration phase transition for strange quarks is a little larger than that for light quarks in the PNJL model due to the larger current quark mass of strange quarks [38], and locations of the cusp of the quartic fluctuations and the oscillation of the 6th order fluctuations for strange quarks is related with this pseudo-critical temperature for strange quarks, which is about $1.2T_C$ in the PNJL model. On the contrary, results obtained in lattice calculations in Ref. [28] indicate that the pseudo-critical temperature of the strange quark chiral phase transition is same as that for light quarks. However, we should emphasize that in some other lattice simulations, for example in Ref. [22], these two pseudo-critical temperatures are different and the pseudo-critical temperature for strange quarks is larger than that for light quarks. Furthermore, because of the effects of current quark masses in the PNJL model, especially for the strange quarks, fluctuations obtained in the PNJL model approaches to their corresponding Stefan-Boltzmann values more slowly than those obtained in lattice calculations. Comparing the fluctuations of electric charge with those of baryon number, we find that the former calculated in the PNJL model are better consistent

with those obtained in lattice calculations than the latter, since the fluctuations of electric charge have more contributions from light quarks than the fluctuations of baryon number. Although the conclusion about whether there is a cusp during the phase transition in the ratio of quartic to quadratic fluctuations of the baryon number, i.e. χ_4^B/χ_2^B , is not clear in lattice calculations due to the large errors in their simulations, We indeed find a pronounced cusp in this ratio χ_4^B/χ_2^B at the critical temperature in our calculations, which confirms that χ_4^B/χ_2^B is a valuable probe of the deconfinement and chiral phase transitions.

Furthermore, we have also studied the correlations among conserved charges in the PNJL model and compared our calculated results with those obtained in lattice simulations. Same as the fluctuations of conserved charges, except for some small quantitative differences, these correlations among conserved charges calculated in the PNJL model are well consistent with those obtained in the lattice calculations.

Acknowledgements

This work was supported by the National Natural Science Foundation of China under Contract Nos. 10425521, 10675007, and 10935001, and the Major State Basic Research Development Program under Contract No. G2007CB815000. One of the authors (W. J. F.) also acknowledges financial support from China Postdoctoral Science Foundation No. 20090460534.

-
- [1] E. V. Shuryak, Prog. Part. Nucl. Phys. **53**, 273 (2004).
 - [2] M. Gyulassy, and L. McLerran, Nucl. Phys. **A 750**, 30 (2005).
 - [3] E. V. Shuryak, Nucl. Phys. **A 750**, 64 (2005).
 - [4] I. Arsene *et al*, Nucl. Phys. **A 757**, 1 (2005).
 - [5] B. B. Back *et al*, Nucl. Phys. **A 757**, 28 (2005).
 - [6] J. Adams *et al*, Nucl. Phys. **A 757**, 102 (2005).
 - [7] K. Adcox *et al*, Nucl. Phys. **A 757**, 184 (2005).
 - [8] J.-P. Blaizot, J. Phys. **G 34**, S243 (2007).
 - [9] F. Weber, Prog. Part. Nucl. Phys. **54**, 193 (2005).

- [10] M. Alford, D. Blaschke, A. Drago, T. Klähn, G. Pagliara, J. Shaffner-Bielich, *Nature* **445**, E 7 (2007).
- [11] M. Alford, A. Schmitt, K. Rajagopal, and T. Schäfer, *Rev. Mod. Phys.* **80**, 1455 (2008).
- [12] W. J. Fu, H. Q. Wei, and Y. X. Liu, *Phys. Rev. Lett.* **101**, 181102 (2008).
- [13] G. Boyd, J. Engels, F. Karsch, E. Laermann, C. Legeland, M. Lügemeier, and B. Petersson, *Nucl. Phys.* **B 469**, 419 (1996); J. Engels, O. Kaczmarek, F. Karsch, and E. Laermann, *Nucl. Phys.* **B 558**, 307 (1999).
- [14] Z. Fodor, and S. D. Katz, *Phys. Lett.* **B 534**, 87 (2002); *ibid*, *J. High Energy Phys.* **0203**, 014 (2002); Z. Fodor, S. D. Katz, and K. K. Szabo, *Phys. Lett.* **B 568**, 73 (2003).
- [15] C. R. Allton, S. Ejiri, S. J. Hands, O. Kaczmarek, F. Karsch, E. Laermann, Ch. Schmidt, and L. Scorzato, *Phys. Rev.* **D 66**, 074507 (2002); C. R. Allton, S. Ejiri, S. J. Hands, O. Kaczmarek, F. Karsch, E. Laermann, and Ch. Schmidt, *Phys. Rev.* **D 68**, 014507 (2003); C. R. Allton, M. Döring, S. Ejiri, S. J. Hands, O. Kaczmarek, F. Karsch, E. Laermann, and K. Redlich, *Phys. Rev.* **D 71**, 054508 (2005).
- [16] E. Laermann, and O. Philipsen, *Ann. Rev. Nucl. Part. Sci.* **53**, 163 (2003).
- [17] P. de Forcrand, and O. Philipsen, *Nucl. Phys.* **B 642**, 290 (2002); **B 673**, 170 (2003); P. de Forcrand, and S. Kratochvila, *Nucl. Phys. B, Proc. Suppl.* **153**, 62 (2006).
- [18] S. Kratochvila, and P. de Forcrand, *Nucl. Phys. B, Proc. Suppl.* **129**, 533 (2004); **140**, 514 (2005); *Phys. Rev.* **D 73**, 114512 (2006).
- [19] R. V. Gavai, and S. Gupta, *Phys. Rev.* **D 72**, 054006 (2005).
- [20] R. V. Gavai, and S. Gupta, *Phys. Rev.* **D 73**, 014004 (2006).
- [21] Y. Aoki, G. Endrodi, Z. Fodor, S. D. Katz, and K. K. Szabó, *Nature* **443**, 675 (2006).
- [22] Y. Aoki, Z. Fodor, S. D. Katz, and K. K. Szabó, *Phys. Lett.* **B 643**, 46 (2006).
- [23] M. Cheng *et al.*, *Phys. Rev.* **D 74**, 054507 (2006).
- [24] S. Ejiri, F. Karsch, and K. Redlich, *Phys. Lett.* **B 633**, 275 (2006).
- [25] S. Ejiri *et al.*, *Nucl. Phys.* **A 774**, 837 (2006).
- [26] F. Karsch, S. Ejiri, and K. Redlich, *Nucl. Phys.* **A 774**, 619 (2006).
- [27] F. Karsch, *PoS CPOD07*, 026 (2007).
- [28] M. Cheng *et al.*, *Phys. Rev.* **D 79**, 074505 (2009).
- [29] S. Ejiri *et al.*, arXiv:0909.5122 [hep-lat].
- [30] M. A. Stephanov, K. Rajagopal, and E. V. Shuryak, *Phys. Rev. Lett.* **81**, 4816 (1998).

- [31] Y. Hatta, and T. Ikeda, Phys. Rev. **D 67**, 014028 (2003).
- [32] S. Jeon, and V. Koch, in: R. C. Hwa, X. N. Wang (Eds.), Quark Gluon Plasma, vol. 3, World Scientific Publishing, 2004, p.430.
- [33] M. Stephanov, Acta Phys. Pol. B **35**, 2939 (2004).
- [34] S. Jeon, and V. Koch, Phys. Rev. Lett. **85**, 2076 (2000).
- [35] V. Koch, A. Majumder, and J. Randrup, Phys. Rev. Lett. **95**, 182301 (2005).
- [36] B. Stokić, B. Friman, and K. Redlich, Phys. Lett. **B 673**, 192 (2009).
- [37] B. I. Abelev *et al.* (STAR Collaboration), Phys. Rev. Lett. **103**, 092301 (2009).
- [38] W. J. Fu, Z. Zhang, and Y. X. Liu, Phys. Rev. **D 77**, 014006 (2008).
- [39] P. N. Meisinger, and M. C. Ogilvie, Phys. Lett. **B 379**, 163 (1996); P. N. Meisinger, T. R. Miller, and M. C. Ogilvie, Phys. Rev. **D 65**, 034009 (2002).
- [40] R. D. Pisarski, Phys. Rev. **D 62**, 111501 (2000); A. Dumitru and R. D. Pisarski, Phys. Lett. **B 504**, 282 (2001); Phys. Lett. **B 525**, 95 (2002); Phys. Rev. **D 66**, 096003 (2002).
- [41] K. Fukushima, Phys. Lett. **B 591**, 277 (2004).
- [42] C. Ratti, M. A. Thaler, and W. Weise, Phys. Rev. **D 73**, 014019 (2006).
- [43] S. Rößner, C. Ratti, and W. Weise, Phys. Rev. **D 75**, 034007 (2007).
- [44] M. Ciminale, R. Gatto, N. D. Ippolito, G. Nardulli, and M. Ruggieri, Phys. Rev. **D 77**, 054023 (2008).
- [45] Z. Zhang, and Y. X. Liu, Phys. Rev. **C 75**, 064910 (2007) (arXiv: hep-ph/0610221).
- [46] W. J. Fu, and Y. X. Liu, Phys. Rev. **D 79**, 074011 (2009).
- [47] S. K. Ghosh, T. K. Mukherjee, M. G. Mustafa, and R. Ray, Phys. Rev. **D 73**, 114007 (2006); S. Mukherjee, M. G. Mustafa, and R. Ray, Phys. Rev. **D 75**, 094015 (2007)
- [48] P. Rehberg, S. P. Klevansky, and J. Hüfner, Phys. Rev. **C 53**, 410 (1996).
- [49] C. Amsler *et al.* (Particle Data Group), Phys. Lett. **B 667**, 1 (2008).
- [50] F. Karsch, K. Redlich, and A. Tawfik, Phys. Lett. **B 571**, 67 (2003).